



LUND UNIVERSITY

Influence of excited state Pr^{3+} on the relaxation of the Pr^{3+} - YAlO_3 3H4-1D2 transition

Kröll, Stefan; Xu, E.; Kachru, R.

Published in:
Physical Review B (Condensed Matter)

DOI:
[10.1103/PhysRevB.44.30](https://doi.org/10.1103/PhysRevB.44.30)

1991

[Link to publication](#)

Citation for published version (APA):
Kröll, S., Xu, E., & Kachru, R. (1991). Influence of excited state Pr^{3+} on the relaxation of the Pr^{3+} - YAlO_3 3H4-1D2 transition. *Physical Review B (Condensed Matter)*, 44(1), 30-34. <https://doi.org/10.1103/PhysRevB.44.30>

Total number of authors:
3

General rights

Unless other specific re-use rights are stated the following general rights apply:
Copyright and moral rights for the publications made accessible in the public portal are retained by the authors and/or other copyright owners and it is a condition of accessing publications that users recognise and abide by the legal requirements associated with these rights.

- Users may download and print one copy of any publication from the public portal for the purpose of private study or research.
- You may not further distribute the material or use it for any profit-making activity or commercial gain
- You may freely distribute the URL identifying the publication in the public portal

Read more about Creative commons licenses: <https://creativecommons.org/licenses/>

Take down policy

If you believe that this document breaches copyright please contact us providing details, and we will remove access to the work immediately and investigate your claim.

LUND UNIVERSITY

PO Box 117
221 00 Lund
+46 46-222 00 00

Influence of excited-state Pr^{3+} on the relaxation of the $\text{Pr}^{3+}:\text{YAlO}_3$ 3H_4 - 1D_2 transition

S. Kröll

Department of Physics, Lund Institute of Technology, P.O. Box 118, S-221 00 Lund, Sweden

E. Y. Xu* and R. Kachru

Molecular Physics Laboratory, SRI International, Menlo Park, California 94025

(Received 21 November 1990)

Two-pulse photon-echo measurements on the 0.1 at. % $\text{Pr}^{3+}:\text{YAlO}_3$ 3H_4 - 1D_2 transition suggest that the relaxation time depends on the density of excited states created by the excitation pulses. The dependence of the relaxation time on the intensity of each excitation pulse shows that our results are inconsistent with instantaneous spectral diffusion, a model often invoked in this type of experiment, where excited states created by the second pulse chiefly influence the relaxation time. A homogeneous linewidth contribution, noted in previous work as being of unknown origin, is eliminated at low excitation fluences.

There is currently considerable interest in understanding and modeling relaxation processes such as ion-ion and ion-lattice interactions, in rare-earth-ion-doped crystals at low temperatures both from a fundamental point of view and for potential applications.¹⁻⁶ Coherent optical transient techniques are commonly used for retrieving information on the dynamic processes in such crystals, and recently the effect of excitation pulse intensity and energy on the observed dephasing process has been brought to attention.⁷⁻¹⁴ For the free induction decay (FID), an extrapolation to zero excitation intensity is necessary for extracting the homogeneous linewidth for the material studied. Such extrapolations were often compared with a photon-echo measurement to ascertain that the correct value was obtained.^{11,15} There is, however, now increasing evidence that, at least for the rare-earth-doped crystals, the energy and intensity of the excitation pulses also affects the linewidth and dephasing time measured using photon echoes.^{7-10,12-14} Generally, this intensity dependence is ascribed to instantaneous spectral diffusion¹⁶⁻¹⁸ where states excited by the second pulse destroy the rephasing of the echo signal. A very clear demonstration of such a case was recently presented.¹⁰

In this paper we describe an excitation-energy-dependent relaxation mechanism for the 3H_4 - 1D_2 transition in 0.1 at. % $\text{Pr}^{3+}:\text{YAlO}_3$,¹² which, contrary to the recent investigations in $\text{Eu}^{3+}:\text{Y}_2\text{O}_3$ (Refs. 7 and 10) and $\text{Tb}^{3+}:\text{LiYF}_4$,¹² cannot be explained in terms of instantaneous spectral diffusion. At low excitation energies the measured homogeneous linewidth for this transition is far narrower than that observed in previous experiments, and we suggest that a previously unidentified contribution to the homogeneous linewidth^{1,19} is due to the excitation-energy-dependent effect studied in the present work.

The experimental setup consists of a Coherent Radiation CR699-21 ring dye laser pumped by a Coherent Ra-

diation Innova-200 argon-ion laser. The two-pulse excitation sequence is produced by gating an acousto-optic modulator (AOM) and focused into the $\text{Pr}^{3+}:\text{YAlO}_3$ crystal, which is immersed in a liquid-helium cryostat. The sample was normally kept at a temperature of 4.6 K, but decay rates were the same at 4.6 and 2 K for high as well as low excitation energies. A Pockels cell between crossed polarizers is gated to transmit the photon echo generated by the excitation sequence to the RCA C31034 photomultiplier tube (PMT). A second Pockels cell inserted between parallel polarizers in front of the cryostat is gated at the same time, closing the beam path between the AOM and the cryostat and thus blocking the continuous-wave (cw) leakage through the AOM before it reaches the PMT during the echo-detection sequence.²⁰ The PMT signal is processed by a gated boxcar integrator. Data collection and timing between the AOM, Pockels cells, and boxcar is performed by a PDP 11 computer through two digital-delay generators (Stanford Research System DG535).

The excitation pulses were attenuated either by neutral-density filters or by reducing the output voltage of the delay generator gating the AOM driver. In contrast to merely changing the gating voltage at the input of AOM driver, the neutral-density filters also attenuated the cw leakage that reached the sample between pulses, and this approach was therefore used at the very lowest excitation pulse energies. These two methods of attenuating the excitation pulses, however, produced the same echo-relaxation time T_2 within 10%. Thus the cw leakage ($< 50 \mu\text{W}$ at the crystal) did not appear to have any significant effect on the dephasing time at high or intermediate pulse energies in this experiment. Figure 1 shows an experimental recording of the photon-echo signal as a function of delay between excitation pulses, together with a least-squares fit with the assumption of exponential decay of the photon-echo signal. All the data in this work were fit to the equation $I_e = I_0 \exp(-4\tau/T_2)$,

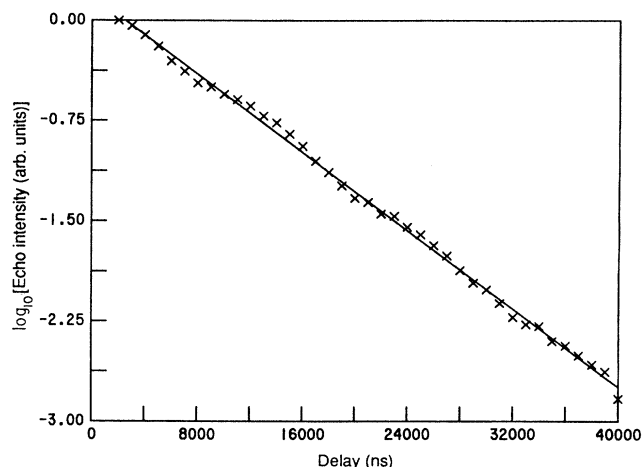


FIG. 1. Experimental two-pulse photon-echo decay together with a fit with the assumption of exponential decay, yielding $T_2 = 24 \mu\text{s}$.

where I_e is the echo intensity. Although the echo-decay curves, in general, were slightly nonsimple exponentials, as a function of τ , all the data points could be fitted to a simple exponential decay to within $\pm 5\%$. The solid line in Fig. 1 is obtained with $T_2 = 24 \mu\text{s}$.

Figure 2(a) shows the logarithm of T_2 for the ${}^3H_4-{}^1D_2$ transition in 0.1 at. % $\text{Pr}^{3+}:\text{YAlO}_3$ as a function of the logarithm of the sum of the energy in the two excitation pulses. Depending on excitation pulse energy, it is possible to measure both significantly longer and significantly shorter relaxation times than the $35\text{-}\mu\text{s}$ value reported previously.¹ The duration of the excitation pulses was normally set to 900 ns. The triangles in Fig. 2 represent measurements where the first and second pulses have the same excitation energy. The solid (open) squares represent the photon-echo relaxation measurements when the first (second) excitation pulse has higher energy than the second (first) pulse. In Fig. 2(b), T_2 is plotted as a function of first-pulse excitation energy and in Fig. 2(c) as a function of second-pulse excitation energy. Thus, on the left-hand side in Figs. 2(b) and 2(c), the variation of photon-echo decay time T_2 when one of the excitation pulses (first or second) is kept fixed at a low energy, while the energy of the other excitation pulse is increased, can be seen. The solid line in Fig. 2(b) shows the T_2 for a weak second pulse, calculated from a semiquantitative analysis using the instantaneous-spectral-diffusion (ISD) model, described below.

The physical mechanism for the change of dephasing time due to ISD (Refs. 9, 10, 12, 16, 17, and 21) is that excitation (or deexcitation) of a dopant ion changes its permanent electric (or magnetic) dipole moment, which causes a change of the local crystal field in the vicinity of the ion. This change of field may cause the transition frequency of any nearby ion to change. If this change occurs while this second ion participates in the generation of a photon echo, the rephasing of this second ion will no longer occur at the echo time and the echo signal will decrease. For ISD a strong second pulse has a larger

effect on the echo-relaxation time than a strong first pulse because a change in crystal field induced by the first pulse only changes the inhomogeneous absorption frequencies and does not destroy the photon-echo rephasing. Huang

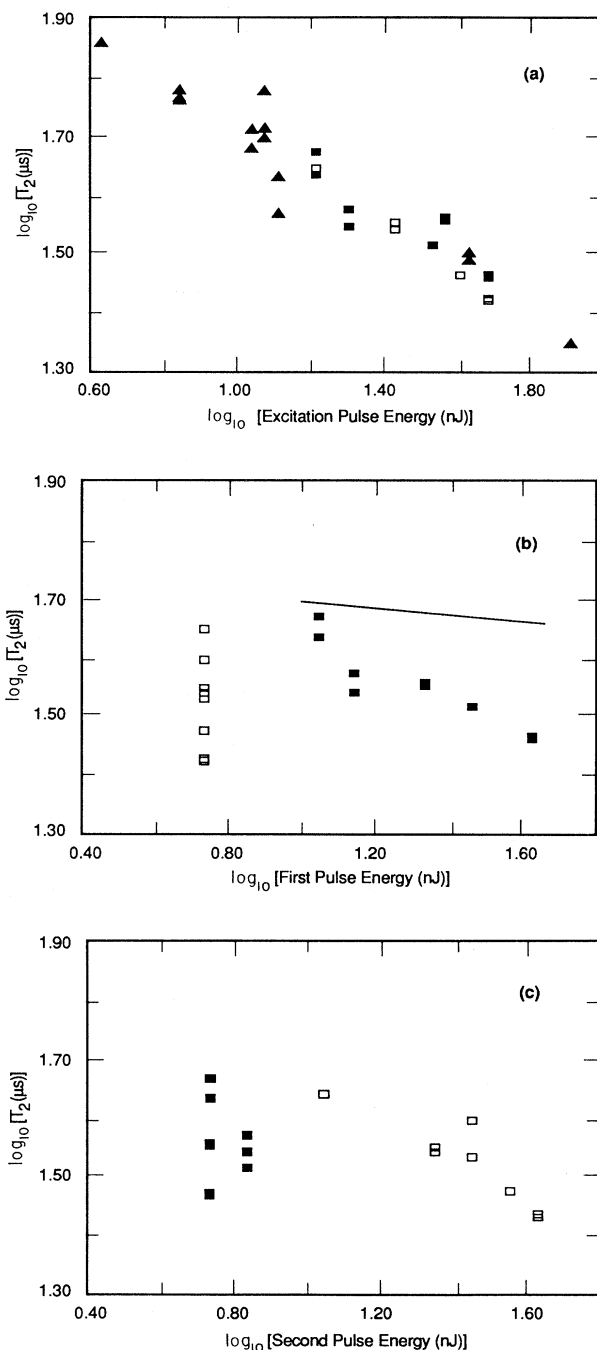


FIG. 2. Triangles represent points where first and second excitation pulse has the same energy, solid squares where the first pulse has larger energy, and open squares points where the second pulse has larger energy. The x axis is (a) the sum of the energy in the two excitation pulses, (b) the energy of the first pulse, and (c) the energy of the second pulse. Solid line in (b) is a prediction of T_2 when the second pulse has the lowest energy based on the instantaneous spectral diffusion model.

*et al.*¹⁰ observed approximately a factor of 10 shorter T_2 , with a strong second excitation pulse than with a strong first pulse. If the radiative lifetime (T_R) of the upper state is known, the decrease of T_2 due to a strong first pulse can be estimated from the decrease due to a strong second pulse with the assumption that the ISD mechanism is responsible for the change in T_2 .^{9,10} Using the approach described in Ref. 9, the line in Fig. 2(b) is the ISD prediction of T_2 versus first-pulse energy calculated²² from the values with a strong second pulse and with the assumption that T_R is 185 μs .¹ As can be seen from Fig. 2(b), the ISD model fails to predict the dependence of T_2 on first-pulse energy.

In an attempt to parametrize T_2 as a function of photon-echo signal size, we repeatedly performed measurements in which either the first or second excitation pulse was one or two orders of magnitude smaller than the other pulse. This test gave no indication that the echo-signal size was a relevant parameter for describing the intensity-dependent dephasing. However, for the largest differences in excitation energies, a 10–15 % shorter T_2 was observed for a strong second pulse than for a strong first pulse. This difference is small compared to the factor of 3 difference in T_2 observed in Fig. 2, but it indicates that there may still be a minor contribution to the excitation-energy-dependent dephasing from ISD.

Optically dense samples have also been shown to yield intensity-dependent relaxation times.²³ A simple physical picture of the mechanism leading to this intensity dependence is that in a sample of high optical density a substantial amount of the photons in the excitation pulses (as well as in the echo) will be absorbed during the propagation through the crystal. Ions at the rear end of the crystal will therefore experience a lower-excitation-energy fluence than ions at the face where the excitation pulses enter the crystal.²³ A strong first pulse, however, may saturate the transition; thus the second excitation pulse, as well as the echo, will then experience less attenuation as it propagates through the crystal. For longer delays between the first and second excitation pulse, ions excited by the first (second) pulse will have more time to decay before the second pulse (echo) propagates through the sample, and absorption will therefore increase as a function of delay. This additional mechanism will reduce the photon-echo signal, yielding an apparent decrease of T_2 as a function of excitation energy.²³

To find out whether the observed intensity dependence was due to the optical density effect, we studied two samples, 1 and 0.4 mm long, cut from the same crystal. These samples had optical densities of 1.3 and 0.6, respectively, at the line center of the $^3H_4-^1D_2$ transition. Two observations suggest that the observed intensity-dependent relaxation is not an optical density effect. First, for identical excitation and focusing conditions, the two samples gave the same apparent T_2 within 10%, and second, no significant difference between the slopes in log-log plots of T_2 versus excitation-pulse area could be seen for the two samples. The first part of this test was conducted both with strong excitation pulses, yielding a T_2 of 25 μs , and at lower energies yielding a T_2 of about

50 μs .

Within the range of excitation energies used for any given focusing condition and excitation-pulse temporal width, only the sum of the energy in the two excitation pulses could be used to parametrize variations in T_2 . Not surprising, therefore, the pulse area of the excitation pulses could not be used for the parametrization. This is illustrated in Fig. 3, where in Fig. 3(a) T_2 versus pulse area is shown for excitation pulses of duration 450 ns (squares), 900 ns (crosses), 1800 ns (plus signs), and 3600 ns (diamonds), and in Eq. 3(b), T_2 versus total excitation energy is shown for the same set of data. Pulse areas in the present work were generally kept between $\pi/2$ and $\pi/16$. A fair amount of the measurements could therefore be considered to be in the small-angle limit. Usually, in the small-angle limit, the number density of excited ions is considered to be proportional to the pulse angle. However, as the excitation-pulse duration is made shorter, not only does the pulse area become smaller, but the excitation-pulse bandwidth will also be larger. Therefore, when the bandwidth dependence of short excitation pulses is taken into account, the number density of the

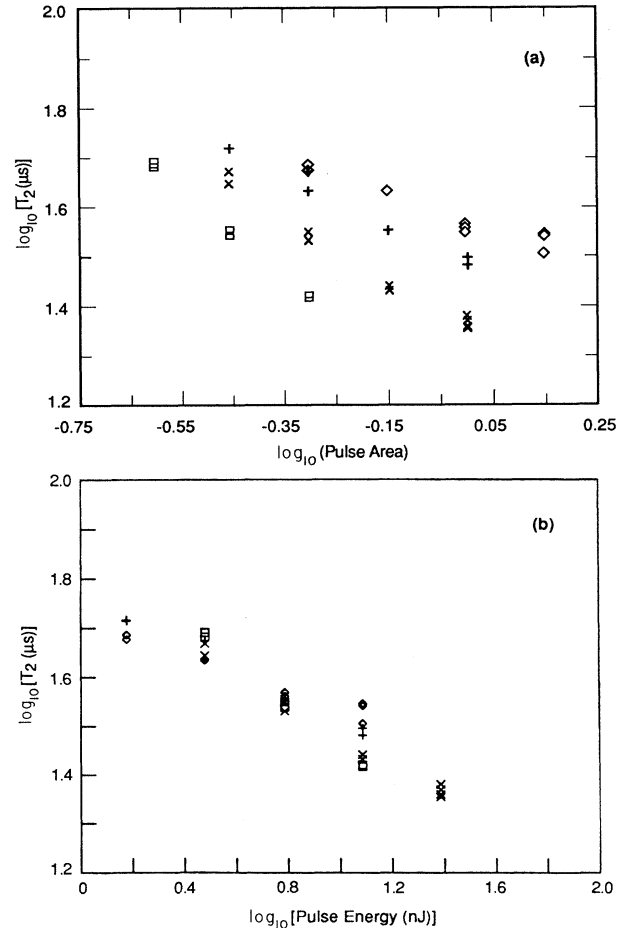


FIG. 3. Logarithm of T_2 vs (a) excitation-pulse area and (b) excitation-pulse energy. Duration of excitation pulses is 450 ns (squares), 900 ns (crosses), 1800 ns (plus signs), and 3600 ns (diamonds).

excited state is no longer directly proportional to the excitation-pulse area.

Based on the recorded data, it appears reasonable to assume that the density of excited states is a critical parameter for the increase in dephasing rate. The fact that excitation far out in the wing of the inhomogeneous line yielded comparatively long T_2 at high excitation energies is also consistent with the assumption that the number of density of excited ions is the important parameter. The bandwidth of the excitation pulses is approximately given by the inverse pulse duration. Although the CR699-21 linewidth is nominally 1 MHz, this is the linewidth measured over time scales of the order of seconds. For a few microseconds the width is much narrower.¹¹ During the time between excitation pulses (here always less than 100 μs), there might be some drift of the laser frequency¹¹ such that the second pulse would not address exactly the same homogeneous subgroup as that excited by the first pulse within the inhomogeneous profile. This drift would then act as an additional decay mechanism shortening T_2 , but this contribution would be intensity independent.

It is surprising that the 0.1 at. % $\text{Pr}^{3+}:\text{YAlO}_3$ sample investigated here appears to have an intensity-dependent dephasing mechanism so different from that in 2 at. % $\text{Eu}^{3+}:\text{Y}_2\text{O}_3$ (Ref. 10) and 1 at. % $\text{Tb}^{3+}:\text{LiYF}_4$.¹² The different behaviors observed could be related to the average distance between excited ions in the different investigations. In the $\text{Pr}^{3+}:\text{YAlO}_3$ crystal, the dopant ion concentration is a factor of 20 lower, the inhomogeneous linewidth is a factor of 2 smaller,¹ and the bandwidth of the (stronger) excitation pulses is two orders of magnitude smaller than in the $\text{Eu}^{3+}:\text{Y}_2\text{O}_3$ work. With the assumption of microscopic inhomogeneous broadening,^{24,25} the average distance between excited ions (or, alternatively, to the nearest excited neighbor) for a given pulse area is then an order of magnitude larger²⁶ in the $\text{Pr}^{3+}:\text{YAlO}_3$ crystal, and compared to the $\text{Tb}^{3+}:\text{LiYF}_4$ (Ref. 12) work, the difference is even larger. Any short-range effects should therefore be less dominant in the present work. An earlier observation of intensity-dependent T_2 on the 3H_4 - 3P_0 transition in 0.01 at. % $\text{Pr}:\text{YAG}$ (Ref. 9) appeared to give a result that could partly be described with the ISD model. Although the effect of an intense first pulse also in Ref. 9 was too strong to be described by the ISD model, the second-pulse intensity still had a significantly larger impact on the dephasing rate than reported here. The bandwidth of the excitation pulses in the $\text{Pr}:\text{YAG}$ work was about a factor of 30 larger than in Ref. 10, and the distance between excited ions would therefore be intermediate between the two cases discussed above. The analysis above is, however, contradicted by the observation in Ref. 7, where the intensity-dependent behavior in $\text{Eu}^{3+}:\text{Y}_2\text{O}_3$ at low densities of excited states was consistent with ISD.

A possible explanation of the excitation-pulse intensity dependence we observe is an intensity-dependent spin-flip rate. The homogeneous broadening of the Pr^{3+} optical transition is caused by the interaction of Pr^{3+} nuclear spin with a time-dependent magnetic field due to neighboring spins. At low temperatures the time-varying magnetic field is produced by the energy-conserving mutual

spin flips of the Al ions. However, the Al spins neighboring the Pr^{3+} are strongly detuned from the bulk Al spin as a result of Pr-Al dipolar interaction.¹⁷ Therefore, the number of neighboring Al spins taking part in mutual spin flips is greatly reduced, leading to the so-called "frozen-core" effect.¹ The Pr-Al spin interaction is an order of magnitude smaller for the excited 1D_2 state, than for the 3H_4 ground state.¹ Therefore, the frozen-core effect is substantially reduced by a substantial population of excited 1D_2 ions, leading to a greater excitation-intensity-dependent mutual spin-flip rate. In this model the intensity dependence of the relaxation rate is due to the production of optically excited Pr^{3+} ions, but unlike the ISD effect, the increased relaxation rate reflects an increased dephasing rate. Furthermore, there is no asymmetry in the effect of the two excitation pulses on the echo-relaxation rate. The magnetic-field data (see below), however, contradict this explanation based on the frozen-core model. It is therefore unlikely that the frozen-core effect is responsible for the intensity-dependent relaxation that we observe.

Figures 2 and 3 cannot directly be extrapolated to zero excitation energy. Generally, the longest T_2 observed was around 70 μs . Specifically, this was T_2 observed using unfocused excitation beams giving an intensity of less than 1 W/cm^2 during the 900-ns pulses. This measurement correspond to a homogeneous linewidth [full width at half maximum (FWHM)] of 4.5 kHz. Previously, the observed homogeneous linewidth γ_{total} of 9 kHz has been divided into 1 kHz from the 185- μs radiative lifetime γ_{rad} , 5 kHz from magnetic-dipole-induced spin flip flops of Al nuclei in the lattice, γ_{mag} , and the remaining 3 kHz attributed to an unknown broadening mechanism γ_u . Thus $\gamma_{\text{total}} = \gamma_{\text{rad}} + \gamma_{\text{mag}} + \gamma_u$. Based on our results, we infer that the last linewidth contribution above can be eliminated using sufficiently low excitation energies. This is supported by measurements at low excitation energies with a small magnetic field (~ 100 G) applied to the sample.²⁰

We have also briefly performed two-pulse photon echoes on the 3H_4 - 1D_2 transition in 0.01 at. % $\text{Pr}^{3+}:\text{YAG}$ using low excitation energies and observed echo-decay times corresponding to a T_2 around 50 μs . Previously, a decay corresponding to a T_2 of 20 μs had been observed in a crystal of concentration 0.15 at. %.^{1,27} A longer T_2 than previously measured values was also observed for $\text{Eu}^{3+}:\text{Y}_2\text{O}_3$ in Ref. 7. The general implication of these observations appears to be that for some samples two-pulse photon echoes using excitation-pulse areas of $\pi/2$ and π will not provide us with the intrinsic homogeneous decay time of the sample. For example, one can see from Fig. 3(a) that the longer excitation pulses with narrow Fourier widths produce longer T_2 values than shorter pulses with the same pulse area. The reason for this is that because of their larger bandwidth, the shorter pulses must excite a larger number of ions to produce a given flip angle for the Bloch vector, and this larger number of excited ions causes additional dephasing.

In conclusion, an excitation-energy-dependent homogeneous dephasing time has been observed on the 3H_4 -

1D_2 transition in 0.1 at. % $\text{Pr}^{3+}:\text{YAlO}_3$. We cannot explain this observation by the instantaneous spectral diffusion effect or as an optical density effect. The change in dephasing rate can, within the range of excitation energies studied, be parametrized as a function of the sum of the energies in the two excitation pulses, but not as a function of pulse area, pulse intensity, photon-echo intensity, or as a function of the energy in one of the excitation pulses only. As in earlier two-pulse photon-echo measurements, and unidentified homogeneous linewidth contribution of nonradiative and nonmagnetic origin appears

to be eliminated by using small excitation-pulse energies. Thus, at the lowest excitation intensities, the homogeneous linewidth observed in this work is smaller than that previously observed for this transition.

Stimulating discussions with Professor M. D. Fayer are gratefully acknowledged. This work was supported by Nippon Telegraph and Telephone Corporation. S.K. acknowledges the support by the Swedish National Board for Technical Development (STU). This research was conducted during a visit by S.K. to SRI International.

*Present address: Department of Electrical Engineering, Stanford University, Stanford, CA 94025.

¹R. M. Macfarlane and R. M. Shelby, in *Spectroscopy of Solids Containing Rare Earth Ions*, edited by A. A. Kaplyanskii and R. M. Macfarlane (Elsevier, New York, 1987), p. 51.

²F. Moshary, R. Kichinsky, R. J. Beach, and S. R. Hartmann, *Phys. Rev. A* **40**, 4426 (1989).

³W. R. Babbitt, A. Lezama, and T. W. Mossberg, *Phys. Rev. B* **39**, 1987 (1989).

⁴I. Ganem, Y. P. Wang, D. Boye, R. S. Meltzer, W. M. Yen, and R. M. Macfarlane, *Phys. Rev. Lett.* **66**, 695 (1991).

⁵A. Szabo and T. Muramoto, *Phys. Rev. A* **37**, 4040 (1988).

⁶*Persistent Spectral Hole-burning: Science and Applications*, edited by W. E. Moerner (Springer-Verlag, Berlin, 1988).

⁷Jin Huang, J. M. Zhang, and T. W. Mossberg, *Opt. Commun.* **75**, 29 (1990).

⁸M. Mitsunaga and N. Uesugi, *Opt. Lett.* **15**, 195 (1990).

⁹S. Kroll, E. Y. Xu, M. K. Kim, M. Mitsunaga, and R. Kachru, *Phys. Rev. B* **41**, 11 568 (1990).

¹⁰Jin Huang, J. M. Zhang, A. Lezama, and T. W. Mossberg, *Phys. Rev. Lett.* **63**, 78 (1989).

¹¹A. Szabo and T. Muramoto, *Phys. Rev. A* **39**, 3992 (1989).

¹²G. K. Liu and R. L. Cone, *Phys. Rev. B* **41**, 6193 (1990).

¹³G. K. Liu, M. F. Joubert, R. L. Cone, and B. Jacquier, *J. Lumin.* **40&41**, 551 (1988).

¹⁴G. K. Liu, M. F. Joubert, R. L. Cone, and B. Jacquier, *J. Lumin.* **38**, 34 (1987).

¹⁵R. G. DeVoe and R. G. Brewer, *Phys. Rev. Lett.* **50**, 1269 (1983).

¹⁶J. R. Klauder and P. W. Anderson, *Phys. Rev.* **125**, 912 (1962).

¹⁷W. B. Mims, in *Electron Para-magnetic Resonance*, edited by S. Geschwing (Plenum, New York, 1972), p. 263.

¹⁸D. R. Taylor and J. P. Hessler, *Phys. Lett.* **50A**, 205 (1974).

¹⁹R. M. Macfarlane, R. M. Shelby, and R. L. Shoemaker, *Phys. Rev. Lett.* **43**, 1726 (1979).

²⁰S. Kröll and R. Kachru (unpublished).

²¹S. Meth and S. R. Hartmann, *Phys. Lett.* **58A**, 192 (1976).

²²Following Refs. 9 and 10, it is assumed that the observed relaxation time $T_2^{\text{obs}}(E_1, E_2)$ is a function of the excitation-pulse energies, which can be expressed as $4/T_2^{\text{obs}}(E_1, E_2) = 4/T_2^0 + \gamma(E_2) + \gamma(E_1)[1 - \exp(-\tau/T_R)]$. τ is an average time separation between the first and second pulses, here chosen to 21 μs (compare Fig. 1). E_1 (E_2) is the energy of pulse 1 (2), and T_2^0 is the dephasing time in the limit of zero excitation energy. With $\Gamma(E_2, E_1) = 4/T_2^{\text{obs}}(E_2, E_1)$, it is straightforward to show that $\Gamma(E_2, E_1) = \Gamma(E_1, E_2) - \exp(-\tau/T_R)[\Gamma(E_1, E_2) - \Gamma(E_1, E_1)]$. The line in Fig. 2(b) is calculated from this last equation.

²³R. W. Olson, H. W. H. Lee, F. G. Patterson, and M. D. Fayer, *J. Chem. Phys.* **76**, 31 (1982).

²⁴L. Root and J. L. Skinner, *Phys. Rev. B* **32**, 4111 (1985).

²⁵J. L. Skinner, B. B. Laird, and L. Root, *J. Lumin.* **45**, 6 (1990).

²⁶The ratio between average distance between excited ions is calculated as $[\frac{20}{2} \times 100]^{1/3} = 10$.

²⁷R. M. Shelby, A. C. Tropper, R. T. Harley, and R. M. Macfarlane, *Opt. Lett.* **8**, 304 (1983).